Pressure Cycling for Purging of Dead Spaces in High-Purity Gas Delivery Systems

Jivaan Kishore and Farhang Shadman
Dept. of Chemical and Environmental Engineering, University of Arizona, Tucson, AZ 85721

Roy Dittler
Substrate Packaging Technology Development (SPTD), Intel Corporation, Chandler, AZ 85248

Carl Geisert
Arizona Fab/Sort Manufacturing (AzFSM), Intel Corporation, Chandler, AZ 85248

DOI 10.1002/aic.14890
Published online June 16, 2015 in Wiley Online Library (wileyonlinelibrary.com)

The purging of stagnant or dead volumes in gas distribution systems is an important method for removing impurities and maintaining cleanliness. A combination of experimental investigation and computational process modeling is used to study the dynamics of impurity removal under variety of purge conditions. The controlled cycling of pressure during purge is found to enhance the cleaning process significantly, particularly in dead spaces. The process simulator was used to develop and analyze a pressure-cyclic purge (PCP) method and understand the conditions that would make PCP advantageous over steady-state purge (SSP). In particular, the effect of geometric factors, impurity surface interactions, flow rate, and cycle characteristics on PCP and its comparison with SSP was studied. The advantage of the PCP method, in terms of both purge time and gas usage, becomes more pronounced in systems with larger number and size of dead spaces and impurities that interact strongly with the surfaces. © 2015 American Institute of Chemical Engineers *AIChE J*, 61: 3973–3980, 2015

Keywords: ultrahigh pure gas distribution, contamination control, adsorption/gas, computational fluid dynamics, transport

Introduction

The contamination of process tools and distribution lines is highly detrimental to quality and yield in semiconductor manufacturing processes. In particular, the purging of contaminants, such as moisture, that adsorb strongly on surfaces has become a challenging issue in the high-volume manufacturing of advanced devices. Understanding the dynamics of impurity propagation in a gas distribution system is a prerequisite to the development of effective contamination control. Leaks and exposure to the atmosphere or other impurities are major inevitable sources of contamination and revenue loss. Consequently, the purging of gas distribution systems is one of the largest uses of ultrahigh purity (UHP) in fabrication plants (fabs) and is associated with the high cost and excessive downtime during system start-ups and recovery from occasional contaminations. As an example, removal of moisture from distribution lines is of particular significance due to its prevalence as a contaminant and its strong adsorption on stainless steel and other system surfaces.[1–4]

The requirement of a cost-efficient purge technique that can be readily applied to complex gas distribution and delivery systems is ever growing.[5] There have been various experimental as well as process modeling studies of moisture transport and surface interactions.[6–8] These studies have primarily focused on conventional steady-state purge (SSP) in distribution lines;[9–14] however, there also have been some studies of potential advantages of transient purge techniques and pressure pulsing, including application for drying down of pellicle system purification[15] and simple electropolished stainless steel (EPSS) pipe system.[16]

Delivery line tubing is one of the major contributors to the total surface area available for moisture adsorption and retention. The kinetic and surface properties of the tubing, in turn, affect the surface interactions of moisture. Dead volumes resulting from capped laterals, branching off from the main headers, accumulate contaminants and pose an additional obstacle to rapid purging. Conventional SSP purge techniques typically use a constant flow rate in the distribution line until a certain target concentration is reached at the outlet. However, the main mechanism of impurity removal from these volumes is desorption from the surface followed by diffusion, which is a slow process; consequently, the overall outgassing of moisture by conventional purge uses a lot of processing time and UHP gas. Development and application of more effective purge techniques would result in environmental gain, process gain, and cost reduction.[17]

This work focuses on the development and analysis of a PCP purging method that would enhance cleaning of the system in general, and dead volumes in particular. This technique

Correspondence concerning this article should be addressed to F. Shadman at shadman@erc.arizona.edu.

would not use heating or application of vacuum and pumping which would make the purge process more difficult, expensive, and risk introducing leakage of impurities into the UHP systems.[18] In particular, the technique would avoid a large reduction of system pressure, or vacuum pumping, because of the risk of impurities back diffusion from outside or contaminated sections into the clean parts of the system.[19]

Experimental Method

Moisture was chosen as the model contaminant due to its prevalence in UHP gas distribution systems and its tenacity against purge. UHP nitrogen gas derived from a cryogenic source was used as the purge/carrier gas for the studies. Three stages of gas purification, using heated metallic-getter purifiers, reduced the moisture concentration in the purge gas to less than 5.16 E −8 mol/m^3 (0.2 ppb). A moisture permeation tube (G.C. Industries) capable of temperature-controlled release of moisture was used for preparing the challenge gas. The flux of moisture at a given temperature and flow rate of carrier gas was used to estimate the concentration of moisture in the challenge stream. This stream was further mixed with UHP nitrogen to dilute and lower moisture concentration in the challenge streams.

Quarter inch 316-L EPSS tubing was used as transfer lines leading to and away from the test section. Since dead spaces in transfer lines become points of accumulation of unknown amounts of moisture, they were minimized in system design and by maintaining a continuous flow of UHP gas. Piping used for the gas delivery system consisted of a 1.93 m (76 in) long main header with an outer diameter of 0.038 m (1.5 in.), and a 1.27 m (50 in.) long capped lateral with an outer diameter of 0.0127 m (0.5 in.). Gas supply was throttled by means of a two-way valve installed upstream of the experimental test bed shown in Figure 1. A flow restrictive orifice was installed downstream of the delivery system to control the pressure rise and fall.

During the PCP experiments, the supply of UHP gas corresponding to each pressurization or depressurization stage to the test bed gas delivery system was regulated by means of a two-way valve. A 10 L mass-flow controller was used to control the flow rate of UHP purge gas which, in conjunction with the orifice, created a steady state pressure of 6.34E5 Pa (92 psig). A typical cyclic purge was operated with pressure swing between 6.34E5 Pa (92 psig) and 2.21E5 Pa (32 psig). Complete depressurization and repressurization between these high and low operating pressures were realized in 180 and 85 s, respectively.

The gas exiting the test bed was analyzed to obtain the time profile of moisture removal from the system. A cavity ring-down spectrometer (CRDS, Tiger Optics LLC) was used to monitor the gas-phase moisture concentration at the outlet of the test bed with time. The CRDS has a moisture detection range between 5.16 E −8 and 1.29 E −3 mol/m^3 (200 ppt–5000 ppb), with sensitivity of 2.58 E −8 mol/m^3 (100 ppt).

The experiments were carried out in two stages: challenge (introduction of moisture to the delivery system) and purge (drying down the system from known moisture saturation). The test bed was purged with UHP nitrogen to achieve a certain baseline concentration prior to any experimental run to remove adsorbed moisture from surface sites. The system was then challenged with a known concentration of moisture once a baseline was established. In a conventional SSP experiment, a constant flow rate of gas was maintained to purge the system once the system was saturated with a known concentration of moisture. Cycling between two pressure states in a PCP was

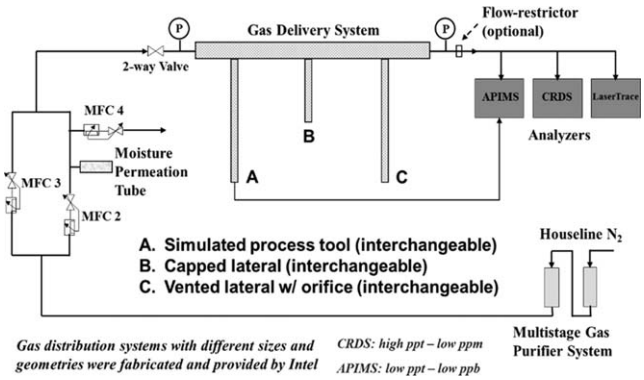

Figure 1. Test bed for study of SSP and PCP.

achieved through valve operation. Depressurization from a high pressure stage is initiated by closing the two-way valve releasing the gas trapped in the system to the analyzer. After the system reached a set low pressure, the valve was opened completely to repressurize the system to a high pressure state. A variety of purge schemes were used to analyze purge performance. These schemes comprised conventional SSP, PCP, and a hybrid combination of SSP and PCP.

Model Development

To analyze the data and study the effects of various system and operational parameters, a comprehensive process model was developed. This model includes the fluid dynamics, mass transport, and species balance, as well as surface interactions between contaminant and delivery lines. To illustrate the basic model formulation, its application to the experimental test bed used in this study is shown in Figure 2. A two-way valve at the inlet controls the flow, and a flow restrictive orifice at the end of the main section controls the depressurization. Further, in order to effectively simulate a purge process, the lateral end is capped to resemble a dead volume.

During PCP, the system is cycling between high- and low-pressure states, differing from a conventional SSP, which stays at a constant pressure and a set flow rate. A typical cycle in a PCP process consists of two steps, namely depressurization and repressurization. The velocity and pressure fields for each step of the PCP cycle are computed by simultaneously solving the continuity and Navier–Stokes equations. The momentum and continuity equations for flow in a pipe are represented by Eqs. 1 and 2.[20] The single-phase Newtonian model was approximated using a weakly compressible flow assumption

$$\frac{\partial \mathbf{A}\boldsymbol{\rho}}{\partial \mathbf{t}} + \nabla \cdot (\mathbf{A}\boldsymbol{\rho}\boldsymbol{u}) = 0 \tag{1}$$

$$\boldsymbol{\rho}\frac{\partial \boldsymbol{u}}{\partial \mathbf{t}} = -\nabla \mathbf{P} - \mathbf{f_D}\frac{\boldsymbol{\rho}}{2\mathbf{d_h}}\boldsymbol{u}|\boldsymbol{u}| \tag{2}$$

The second term on the RHS of Eq. 2 denotes the pressure drop due to viscous shear stress, where, d_h is the hydraulic diameter (proportional to the ratio of cross-sectional area to the wetted perimeter of the pipe section), f_D is the Darcy friction factor accounting for the continuous pressure drop due to viscous shear and is expressed as a function of ratio of surface roughness to hydraulic diameter and Reynolds number at a certain time and location in the system geometry. The surface roughness was assumed to be 25.4 μm for 316 L EPSS. Since most studies were carried out in the Reynolds number ranging in the near laminar

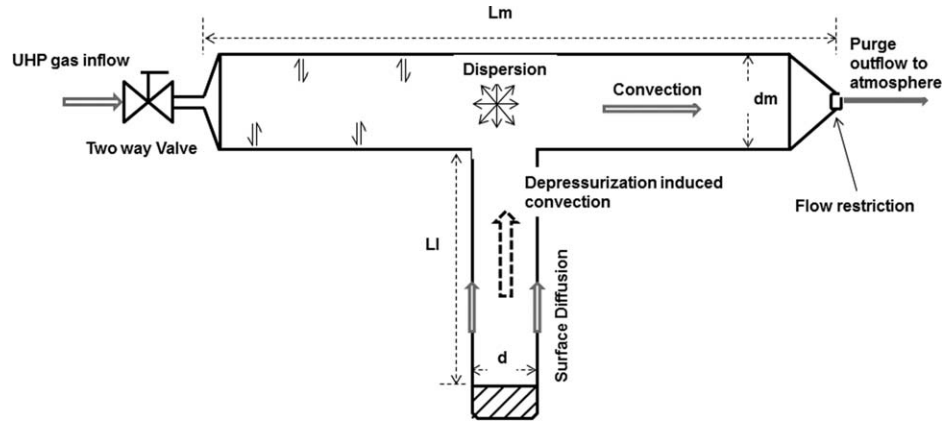

Figure 2. Model schematic and impurity transport mechanisms in a generic gas distribution system.

and transition region, the Churchill friction factor was used. The Churchill equation for single phase fluids given by Eq. 3 can be used for a wide range of ε/d (surface roughness to diameter ratio) and applied over Reynolds numbers in laminar, transition, and turbulent regions.[21] The velocity and concentration profiles during rise and decay in system pressure were compared with using von Karman and Swamee-Jain friction factor models. This served as a test for the accuracy of the numerical solutions and the variability was found to be less than 2%

$$\mathbf{f_D} = 8\left[\left(\frac{8}{\mathbf{Re}}\right)^{12} + (\mathbf{M}+\mathbf{N})^{-1.5}\right]^{\frac{1}{12}} \tag{3}$$

$$\mathbf{M} = \left[-2.457\ln\left[\left(\frac{7}{\mathbf{Re}}\right)^{0.9} + 0.27\frac{\boldsymbol{\varepsilon}}{\mathbf{d}}\right]\right]^{16} \tag{4}$$

$$\mathbf{N} = \left(\frac{37530}{\mathbf{Re}}\right)^{16} \tag{5}$$

The distribution of the contaminant concentration in the gas phase is governed by Eq. 6, where A and Q are the cross-sectional area and total pipe wall surface area per unit volume of the pipe. Flow velocity given by, $\boldsymbol{u} = \mathrm{u}\cdot\boldsymbol{e_t}$ is taken as an input from the simultaneous solution of the momentum and continuity equations, where e_t is the tangential unit vector. A conservative form of the convective term is used in order to fully capture the change in contaminant concentration due to rapid changes in pressure and velocity during pressure cycling. The Langmuir adsorption model is used to characterize the interactions of moisture with pipe surfaces. The kinetic parameters k_a, k_d, and S_0 are characteristic of contaminant species and pipe surface interaction; they are dependent on temperature, carrier gas, contaminant species, and pipe properties such as surface roughness

$$\frac{\partial \mathbf{C_g}}{\partial \mathbf{t}} + \mathbf{A}\nabla.\left(\boldsymbol{u}\mathbf{C_g}\right) = \nabla.\left(\mathbf{A}\mathbf{D_e}\nabla\mathbf{C_g}\right) + \mathbf{Q}\left[\left(\mathbf{k_d}\mathbf{C_s} - \mathbf{k_a}\mathbf{C_g}(\mathbf{S_0}-\mathbf{C_s})\right)\right] \tag{6}$$

Convective and dispersive modes of transport are considered along with volume-averaged flux from surface reactions at the boundary to predict the temporal concentration profiles as purge proceeds. The effective dispersion coefficient in the laminar flow regime is given by the Aris-Taylor dispersion model[22] in Eq. 7

$$\mathbf{D_e} = \mathbf{D_{mp}} + \frac{\mathbf{d}^2\boldsymbol{u}^2}{196\mathbf{D_{mp}}} \tag{7}$$

The molecular diffusivity of a species in a given bulk gas at a certain pressure is related to the diffusivity of the species at atmospheric pressure according to the Chapman-Enskog in Eq. 8

$$\mathbf{D_{mp}} = \frac{\mathbf{D_m}\mathbf{P_{atm}}}{\mathbf{P}} \tag{8}$$

The conservation of surface contaminant concentration relating to gas-phase concentration is given by Eq. 9

$$\frac{\partial \mathbf{C_s}}{\partial \mathbf{t}} = \nabla\cdot(\mathbf{D_s}\nabla\mathbf{C_s}) + \mathbf{k_d}\mathbf{C_s} - \mathbf{k_a}\mathbf{C_g}(\mathbf{S_0}-\mathbf{C_s}) \tag{9}$$

Propagation of moisture on pipe surface through diffusion and reaction with the gas phase determines the distribution of the surface moisture concentration. The diffusivity of moisture in EPSS is given by D_s.

The system is initially pressurized and maintained at a high pressure state $P_{high,}$ with no flow- through the system. The initial surface moisture is considered to be in equilibrium with the initial gas phase moisture concentration as given in Eq. 12.

$$\mathbf{P} = \mathbf{P_{high}} \tag{10}$$

$$\mathbf{C_g} = \mathbf{C_{gi}} \tag{11}$$

$$\mathbf{C_s} = \mathbf{C_{s0}} = \frac{\mathbf{k_a}\mathbf{C_{gi}}\mathbf{S_0}}{\mathbf{k_a}+\mathbf{k_a}\mathbf{C_{gi}}} \tag{12}$$

The pressurization and depressurization of the system is accomplished through a series of valve operations at the inlet. The valve operation along with the resulting sample input pressure profile is shown in Figure 3. The outlet orifice is characterized by a valve loss coefficient K_f. Pressure drop across the valve is calculated from the loss coefficient as given in Eq. 14, where the gas in the main section is assumed to eject to atmospheric pressure.[23] The inlet valve is kept closed for the entire duration of depressurization ($\mathbf{t_d}$). The depressurization period is estimated based on experimental data or characteristic diffusion time of the contaminant species based on the velocity and the length of the dead volume

$$\mathbf{Inlet}: \qquad \mathbf{P} = \mathbf{P_{inlet}}(\mathbf{t}) \tag{13}$$

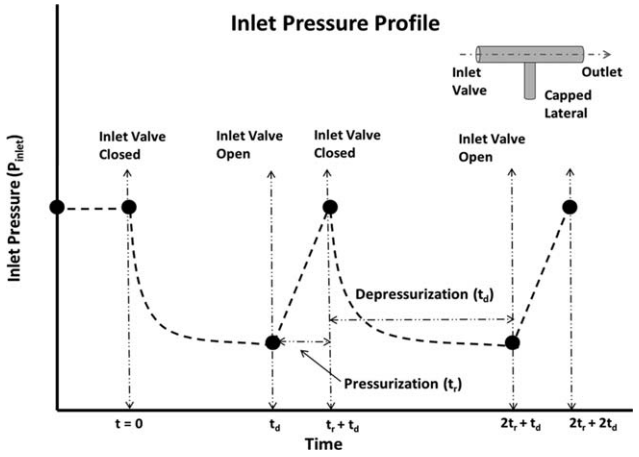

Figure 3. Typical inlet pressure profile during a PCP operation.

$$\textbf{Outlet}: \quad u = \left[\frac{(P - P_{atm})}{K_f \rho}\right]^{0.5} \tag{14}$$

$$\textbf{Lateral}: \quad u = 0 \tag{15}$$

A constant flow of UHP nitrogen gas at a concentration $C_{gin} < 1.29$ E -7 mol/m^3 (0.5 ppb) is maintained during SSP and repressurization stages. The total flux at the lateral end given by Eq. 19 is kept at zero during all stages

$$\textbf{Inlet}:$$

$$\textbf{During pressurization}, \quad C_g = C_{gin} \tag{16}$$

$$\textbf{During depressurization}, \quad \nabla C_g = 0 \tag{17}$$

$$\textbf{Outlet}: \quad \nabla C_g = 0 \tag{18}$$

$$\textbf{Lateral}: \quad -uC_g + D_e \nabla C_g = 0 \tag{19}$$

$$\textbf{All boundaries}: \quad \nabla C_s = 0 \tag{20}$$

The above equations were solved simultaneously using the finite element method (COMSOL Multiphysics). The sections that follow show the results of using this modeling approach to fit the experimental data and determine the kinetic parameters as well as to do case and parametric studies to understand the PCP general features, trends, and potential applications.

Results and Discussion

Model verification and parameter estimation

In order to estimate kinetic parameters including adsorption and desorption rate constants k_a, k_d, and surface site density S_0, the model prediction was fitted to experimental data for an SSP process carried out for 900 s. A good data fit was obtained using $k_a = 7.1E3$ m^3/(mol s), $k_d = 3.78$ E -4 s^{-1}, $S_0 = 1.0$ E -5 mol/m^2. The kinetic parameters estimated correspond to surface interaction of moisture in UHP nitrogen bulk gas with 316 L EPSS surface.

A hybrid SSP-PCP-SSP purge scheme consisting of a 10-cycle PCP with SSP stages prior to and following PCP was used for model verification. The PCP stage cycled between 6.39E5 and 2.39E5 Pa, resulting in an approximate pressure differential of 4.05E5 Pa (4 atm). The SSP stages were carried out at the high-pressure limit at 6.39E5. A comparison of the dry down profile generated from experimental data and model predictions monitoring the gas-phase moisture concentration at the outlet of the main section is shown in Figure 4. The initial delay due to transport time from point of sampling to point of analysis is small and neglected.[24]

The sharp peak at the start of each repressurization stage is a consequence of the density change very close to the flow orifice during rapid pressurization. From equation of continuity and Navier–Stokes, it follows that a sudden increase in the pressure in the main section translates completely to a density gradient. Here, the pressure gradient can be neglected since pressure propagation in the system is very rapid.[25] It is difficult to capture this effect experimentally due to slower data collection rate. Although the model predictions were generated at a 1 s interval, the experimental data was generated every 30 s and is limited by the sampling rate of the analyzer.

An outlet concentration of 1.8 E -6 mol/m^3 (7 ppb) was measured experimentally at the end of a 78-min purge process. This outcome placed the experimental data in good agreement with the model which predicted a final moisture concentration of 2.32 E -6 mol/m^3 (9 ppb), starting from the system of same dimensions and uniform initial concentration of 6.19 E -5 mol/m^3 (240 ppb). It can be seen from the figure that the estimated kinetic constants and fluid dynamic parameters show a good fit for SSP as well as PCP regions.

Comparison of SSP and PCP for moisture removal from dead volumes

The purging of moisture as a contaminant in lateral dead volumes was studied using conventional as well as pressure-cyclic purge (PCP) techniques. The cleanup of point A, as shown in the schematic by the two purge techniques, is shown in Figure 5. The 1 m lateral connected to a 5 m main section is purged by cycling pressure with a high-pressure differential between 8.3E5 and 2.53E5 Pa. Although PCP exhibits a higher purge rate than SSP, the removal of surface adsorbed moisture proceeds at a fairly low rate owing to the low desorption rate constant from EPSS surface.

Parametric study

While the results for moisture clearly show the advantage of PCP over conventional purge, the advantage is expected to increase for impurities which have faster surface interactions (adsorption and desorption) rates; under those conditions the

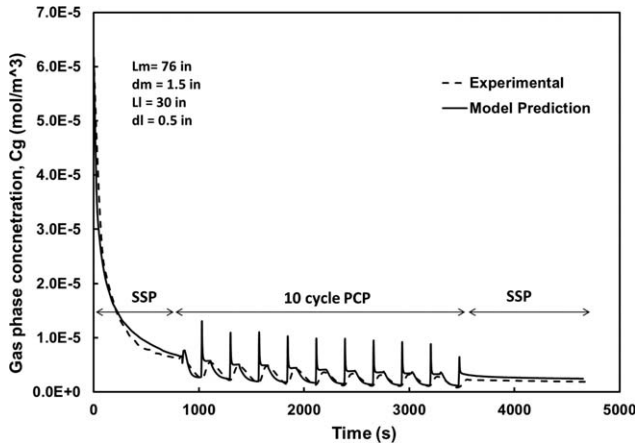

Figure 4. Experimental data fitting and validation of the model.

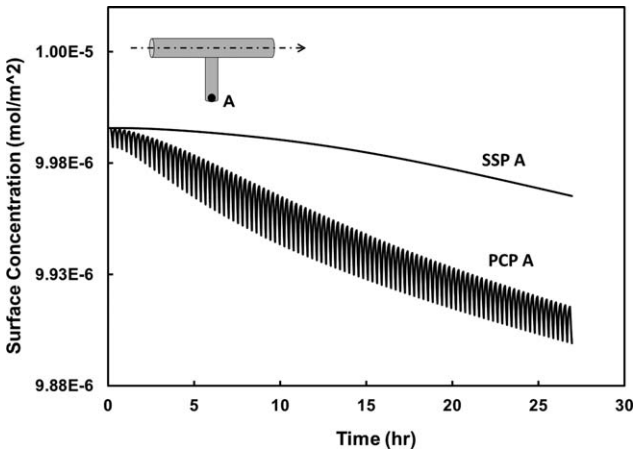

Figure 5. Moisture concentration profile in a dead volume subject to SSP and PCP.

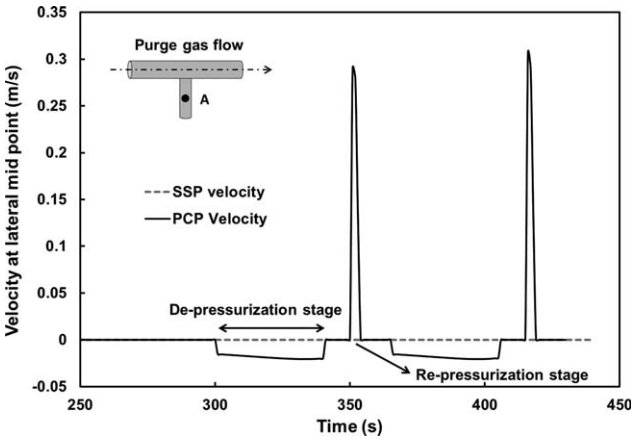

Figure 7. Velocity profiles in the lateral during SSP and PCP.

purge is farther from being controlled by surface interactions and more sensitive to gas-phase transport, and therefore, flow effects. Many impurities are in this class; however, the complete adsorption and desorption rate data (similar to what was measured for moisture, in this study) is not available for almost any impurity of interest. Since the purpose of this study is not generating adsorption/desorption data on various surfaces but is rather a generic study of the features and application of the PCP process, in the parametric study that follows we are using $k_a = 5.0E2\ m^3/(mol\ s)$, $k_d = 5.0\ E\ -2\ s^{-1}$, $S_0 = 1.0\ E\ -6\ mol/m^2$, which are simply a representation of a generic impurity which does not interact with the surface as strongly as moisture and has a lower coverage.

Comparison of PCP and SSP impurity transport and removal mechanisms

A hybrid SSP–PCP–SSP scheme was chosen in order to study the purging of the lateral dead volumes using PCP and its comparison with conventional SSP. The system consisted of a main section of 5 m in length and 0.0381 m in outer diameter, and lateral of length 1 and 0.0127 m in outer diameter located at the midpoint of the main section. The purge profiles presented in Figure 6 show a comparison of the two purge schemes. The surface contaminant concentration was used as an absolute metric to determine the cleanliness of the system. The point being monitored with respect to the UHP gas flow is shown and marked as point "A" in the schematic.

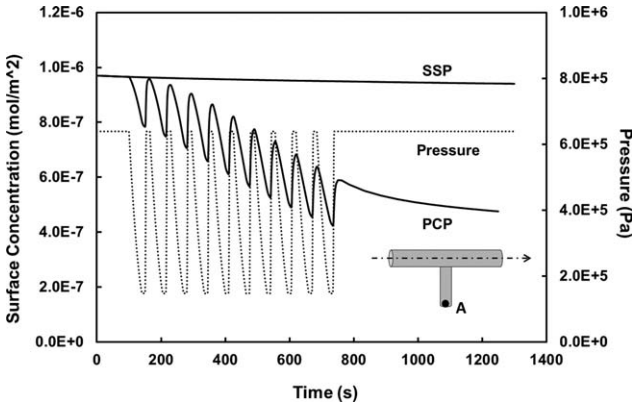

Figure 6. Comparison of SSP and PCP cleanup profiles in the lateral.

SSP runs started with a uniform initial surface concentration of $9.7\ E\ -7\ mol/m^2$ (corresponds to an equilibrium gas-phase concentration of 4 ppm) for approximately three residence times prior to the start of a PCP. This was followed by 21 min (10 cycles) of PCP with high and low pressures of 6.39E5 and 1.52E5 Pa. An orifice loss coefficient of 1E6 was used which allowed a depressurization time of 40 s and rapid repressurization of 4 s. The PCP cycles had holding stages at high and low pressures to improve the efficiency of the purge process. The holding times were predetermined based on the system residence times to allow sufficient removal of contaminants released from the lateral into the main pipe. The above described geometry and operating conditions constitute the base case for further parametric studies.

Figure 7 shows the comparison of the velocity profile of two PCP cycles with that of SSP monitored at a point "A" in the dead volume. During a PCP process, due to the pressure gradient created between the main section and the lateral dead volume, a steady negative velocity, suggestive of a convective flux out of the dead volume, is observed during the depressurization stage. This induced convective flux is the basis of removal of contaminants from the dead volume during a PCP process and is absent in conventional SSP. The additional convective flux out of the lateral dead volume enhances both the dispersive and the convective modes of impurity transport for impurity removal; it also lowers the impurity gas-phase concentration and consequently increases the net rate of desorption. Species transport in the main section is also enhanced, even though that is not usually the bottleneck of the purge process in the systems with dead volumes. Since the primary mode of transport of contaminants from the dead volumes in the SSP is molecular diffusion (bulk and surface), the cleaning effect is orders of magnitude lower and requires long purge time and large quantity of UHP purge gas.

Effect of lateral length and size. A parametric study was conducted on the effect of the PCP technique on systems with varying lateral lengths. A SSP–PCP–SSP purge scheme was implemented on systems with a 5 m main section and 0.2, 1, and 5 m lateral lengths. The results of a 10-cycle PCP are shown in Figure 8. As the lateral length and size increase, the average transport path for impurity out of the lateral increases. Therefore, a higher number of PCP cycles are required to purge the larger dead volume to the same target concentration.

To compare PCP with SSP performance, the ratios of purge time and purge gas usage needed to reach a target surface

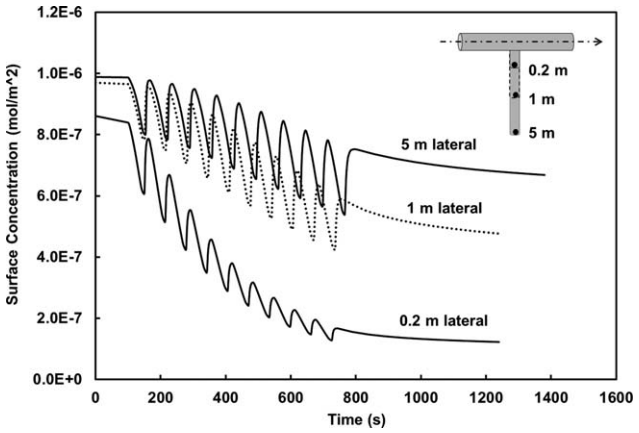

Figure 8. PCP cleanup profiles for three different lateral lengths.

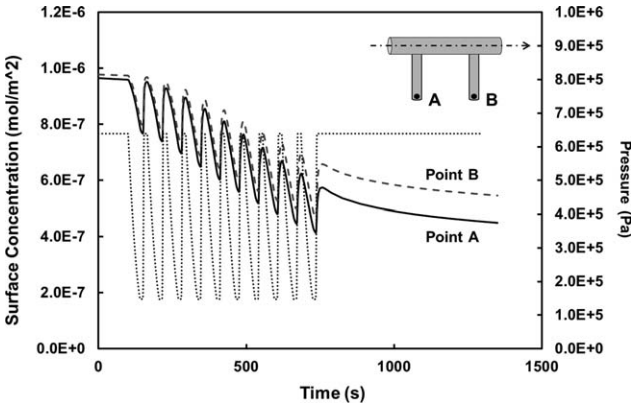

Figure 10. Purge profiles in systems with multiple lateral dead volumes.

concentration, were evaluated. Figure 9 shows the result of this comparison in terms of purge gas usage. Fractional surface cleanup in these figures is the ratio of change in the surface concentration to the initial surface concentration. The purge time and gas usage follow similar trends because of the interdependency of these purge metrics.

Both time and gas usage are key factors in evaluating the performance of a purge process and contribute significantly to the cost and efficiency of the operations. The decrease in purge gas usage to reach a certain target concentration depends on the PCP cycling features (such as high to low pressure ratio and hold time) as well as on the geometry of the system, the flow rates, and the target cleanliness level.

Since dispersion and surface diffusion are the only mechanisms of transport in SSP, the conventional purge approach rapidly loses its relative efficiency as the lateral length increases. With smaller laterals, where the characteristic diffusion length of the contaminants in a given depressurization stage approaches the length of the lateral, the effect of PCP is less pronounced. However, as the lateral length increases, the induced convective flux generated during depressurization stage becomes the dominant mechanism of transport. The relative gas usage and purge time required to reach a certain fractional cleanup decreases drastically as the lateral length increases suggesting that the advantage of PCP is higher with systems with larger dead volumes. Moreover, the relative purge gas and time required by PCP decreases rapidly at higher fractional surface cleanup. As more stringent requirements are placed on the cleanliness of a gas distribution system, higher purge efficiency can be realized with the use of PCP.

Effect of the network complexity and number of laterals. As the complexity of the gas distribution system or number of lateral dead volumes increases, the PCP to SSP advantage increases for reaching a target cleanliness level. To illustrate this point, the effect of the number of lateral dead volumes, a system with a 5-m long main section and 0.038 m in outer diameter with two laterals of 1 m in length and 0.0127 m in outer diameter placed equidistant along the main section, was investigated. A hybrid SSP–PCP–SSP technique with a 10-cycle PCP cycling pressure from 6.39E5 to 1.52E5 Pa was implemented on the system. The other parameters of purge were kept the same as the base case. Figure 10 shows the surface concentration profiles at two points A and B, shown in the schematic.

The lateral dead volume located closer to the outlet of the main section experiences a relatively slower cleanup rate. At any given time during purge, the impurity concentration decreases from main inlet to the outlet. The higher impurity concentration at the opening of the second lateral results in a relatively lower driving force for impurity removal, and therefore, lower overall cleaning rate for the downstream laterals.

Figure 11 compares the relative purge gas usage of PCP to SSP for systems with one and two laterals for a 10-cycle PCP. The results show an increase in the gas savings when the number of laterals increases. This effect is expected to be more pronounced for larger systems. In general, the cleanup of the slower purging points is the limiting factor in determining

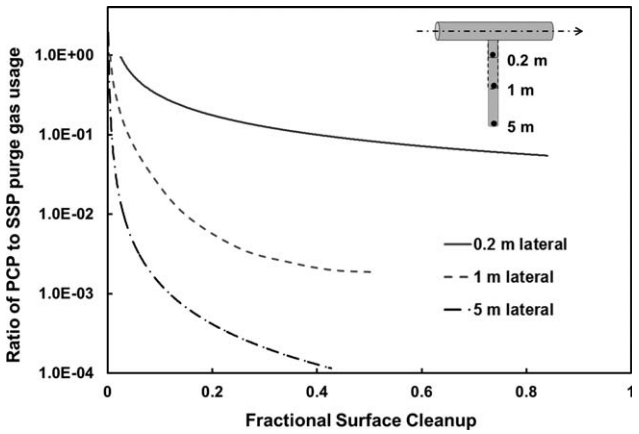

Figure 9. Purge gas usage comparison for PCP and SSP.

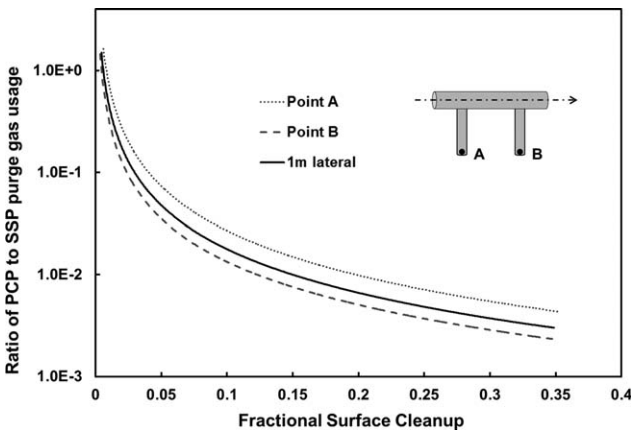

Figure 11. Purge gas savings in systems with multiple lateral dead volumes.

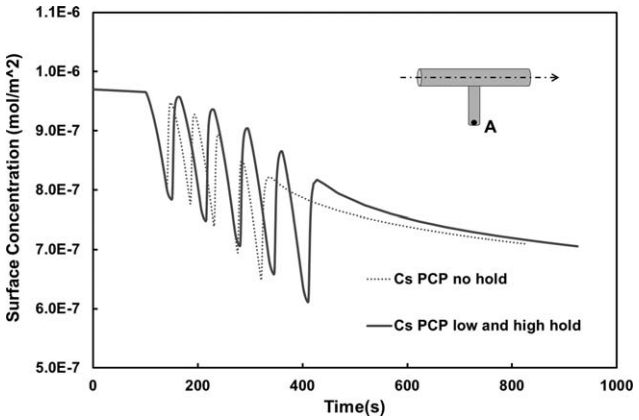

Figure 12. Comparison of PCP schemes with and without hold periods.

purge gas usage or purge time required. The results show that the relative advantage of PCP over SSP increases in the areas that are the cleanup bottleneck such as the downstream dead volumes. Selection of the location for the target cleanup is one important aspect of designing a purge process for a system.

Effect of holding times at high and low pressures. Combining PCP scheme with some SSP hold time was found advantageous for simple straight pipe purge.[16] To analyze the benefit of this hybrid approach in more complex systems, a base case system was subjected to a five-cycle hybrid SSP–PCP–SSP, with initial and final SSP portions of duration 100 and 500 s, respectively. The PCP portion operated between a high pressure of 6.39E5 Pa and low pressure of 2.39E5 Pa with 10 and 15 s hold periods at low and high pressures, respectively. The purge profiles showing the effect of hold stages are shown in Figure 12. The hold times were expected to facilitate the convective removal of impurity in the main section once they enter the main flow from the dead volume. However, the results showed that the presence of hold periods did not in fact increase the purging of a lateral dead volume in reaching the desired target concentration for this geometry. Holding periods seem to help in cases where, due to large dead volumes and/or small flow in the main, there is significant buildup of the impurity transported from the dead volumes in the main. In those cases, the SSP stage in between pressurization and depressurization could enhance the cleanup of the main; however, the enhancement is small compared to the primary gain using PCP instead of SSP.

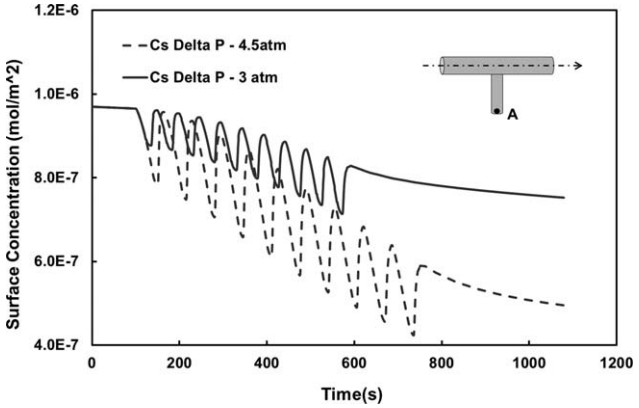

Figure 13. Effect of PCP pressure range on the purge profiles.

Effect of pressure range (Delta P in PCP). In this study, a system with the base case specifications was subject to a hybrid SSP–PCP–SSP scheme; the initial and final SSP portions lasting for 100 and 500 s, respectively. Two runs with 10-cycle PCP with two different pressure ranges were investigated and compared. In one case, the low and high pressure were 1.52E5 and 6.08E5 Pa (Delta $P = 4.56$E5 Pa); in the second case, the low and high pressures were 3.04E5 and 6.08E5 Pa (Delta $P = 3.04$E5 Pa). Figure 13 shows the surface concentration profiles for these two cases. The rate of purge is much higher for the case with the larger pressure range.

The convective flux out of the lateral dead volume during the depressurization stage is the prime factor responsible for the enhanced cleaning effect in PCP. Since this convective flux is generated by the change in pressure, its magnitude depends on the rate and the extent of change in pressure. In general, PCP with higher PCP cycle frequency and larger pressure range will give a higher enhancement in purge. However, the configuration of pipes, valves, and flow control devices as well as the size of a system may put some limitations on the pressure range and cycle frequency that can be practically introduced in a system.

The case studies presented here are not meant to be a search for an optimum or recommended recipe for purge; they are only to show the general differences and trends that show the advantages of PCP over conventional purge. Finding the best purge case for a system is a far more complex multivariable optimization, which requires definition of the desired optimization objectives as well as the degrees of freedom in selecting the system and operation conditions.

Conclusions

A combination of experiments and process simulation was used to study the application of PCP for removal of impurities in gas distribution lines and its comparison with the conventional SSP. The simulator results are in good agreement with the experimental observations and measurements during purging of a gas distribution system with dead volume. The results show that an induced convective flux, generated by pressure changes in PCP, is the primary mechanism that increases the transport of impurities out of the dead volumes and away from the adsorbing surfaces in these areas of contaminant accumulation. The increased cleanup rate results in saving time and purge gas usage needed for the purge process. The enhancement is more pronounced with systems that have laterals and dead volumes; its advantage over conventional SSP increases as the system size and complexity increase.

The simulator can be used to analyze and predict the impurity time and space concentration profiles for both the gas phase and the adsorbed impurities in systems under purge. The model is a useful tool in studying the effects of the parameters that characterize the system, the impurity, and purge operation, and the desired target cleanliness. The key features of PCP, such as the pressure range, the cycle frequency, and the hold time, have significant effect on the enhancement provided by PCP. The optimization of the purge process can be accomplished by means of the process model to build a PCP scheme best suited for a given geometry and operational conditions. This is useful both in the design of the new gas distribution systems and the placement of the flow components, as well as in the cleanup of the existing systems for effective purge application.

Acknowledgments

The authors would like to thank Intel Corporation and Tiger Optics, LLC for providing financial support as well as the donation of test bed parts and the analyzers used in the experiments. The work was also partially supported by the SRC Engineering Research Center for Environmentally Benign Semiconductor Manufacturing at the University of Arizona.

Notations

ε = surface roughness, m
ρ = density of UHP gas, kg m^{-3}
A = cross-sectional area of gas delivery pipeline, m^2
C_g = gas phase concentration, mol m^{-3}
C_{gi} = initial gas phase concentration in equilibrium with moisture in surface, mol m^{-3}
C_{gin} = inlet gas phase concentration of UHP purge gas, mol m^{-3}
C_s = surface moisture concentration, mol m^{-2}
C_{s0} = initial surface concentration in equilibrium with gas phase moisture, mol m^{-3}
D_e = effective dispersion coefficient, m^2 s^{-1}
D_m = molecular diffusion coefficient of moisture in nitrogen at atmospheric pressure P, m^2 s^{-1}
D_{mp} = molecular diffusion coefficient of moisture in nitrogen at pressure P, m^2 s^{-1}
D_s = surface diffusivity of moisture on 316-L EPSS, m^2 s^{-1}
d = diameter of pipe in the experimental test bed, m
d_h = hydraulic radius, m
d_l = diameter of lateral in the experimental test bed, m
d_m = diameter of main header in the experimental test bed, m
e_t = tangential unit vector along the surface of the pipe
f_d = Darcy friction factor
k_a = rate constant of adsorption for moisture on EPSS, m^3 mol^{-1} s^{-1}
k_d = rate constant of desorption for moisture on EPSS, s^{-1}
K_f = characteristic orifice loss coefficient
L_l = length of lateral in the experimental test bed, m
L_m = length of main header in the experimental test bed, m
M, N = terms appearing in Darcy friction factor
P = pressure, Pa
P_{atm} = atmospheric Pressure, Pa
$P_{inlet}(t)$ = inlet pressure profile during pressure cycling, Pa
Q = total pipe wall surface area per unit volume, m^{-1}
Re = Reynolds number
S_0 = density of active surface site, mol m^{-2}
t = time, s
t_d = duration of depressurization stage, s
t_r = duration of repressurization stage, s
u = gas velocity in experimental test bed, m s^{-1}

Abbreviations

EPSS = electro polished stainless steel
PCP = pressure cyclic purge
SSP = steady state purge
UHP = ultrahigh purity
ppb = parts per billion
ppm = parts per million

Literature Cited

1. Haider A, Shadman F. Desorption of moisture from stainless steel tubes and alumina filters in high purity gas distribution systems. *IEEE Trans Compon Hybrids Manufact Technol*. 1991;14(3):507–511.
2. Ishihara Y, Kurihara S, Ishihara S, Toda M, Ohmi T. Trace moisture adsorption onto various stainless steel surface-investigation of adsorption heat and adsorption isotherms. *Hyomen Kagaku*. 1997; 18(9):557–563.
3. Ma C, Verma N. Moisture drydown in ultra-high-purity oxygen systems. *J IEST*. 1998;41(1):13–15.
4. Shadman F, Shero E, Ma C. Fundamentals of moisture interaction with EP stainless steel and silicon wafer surfaces. In: *Institute Of Environmental Sciences And Technology*, 41st Annual Technical Meeting Proceedings, Mount Prospect, IL, 1995:542–548.
5. Pearlstein RM, Berger KR, Hartz CL, Fregger J. Evaluating electronics-grade gas-line purging requirements. *Solid State Technol*. 2001;44(3):119–128.
6. McAndrew JJF, Brandt MD, Li D, Kasper G. Establishing moisture test methods for process gas distribution systems. *Microcontamination*. 1991;9:33–37.
7. Wang HC, Doddi G, Jurcik B, Nishikawa Y. Establishing a particle test sequence for ultra-high-purity gas valves. *Microcontamination*. 1993;11(4):25–33.
8. Siefering K, Whitlock W, Athalye A. Modeling moisture adsorption and transport in ultra-high-purity gas piping systems. *Microcontamination*. 1994;12(3):41–45.
9. Dheandhanoo S, Yang J, Ciotti R, Yesenofski D. Empirical validation of a gas distribution system moisture drydown model. *J IEST*. 1998;41(2):33–38.
10. Dheandhanoo S, Yang JH, Wagner MD. Modeling the characteristics of gas system dry-down. *Solid State Technol*. 2001;6:125–132.
11. Jurcik B, Wang HC, McAndrew J. Dynamic simulation of UHP distribution systems. In: *Microcontamination Conference Proceedings*, San Jose, CA, 1993:222–231.
12. Jurcik B, McAndrew J, Znamensky D. The effect of baking on the dry down of UHP distribution systems: from laboratory to industrial scale via numerical simulation. In: *Institute of Environmental Sciences and Technology, 41st Annual Technical Meeting Proceedings*, Mount Prospect, IL, 1995:557–563.
13. Kubus JM, Leggett GH. Piping system drydown predictions with field verification. In: *Microcontamination Conference Proceedings*, San Jose, CA, 1993:212–221.
14. Yang T, Wu C, Yeh C. Analysis of moisture purge in high purity gas distribution systems. *Int J Heat Mass Transf*. 2006;49(9–10): 1753–1759.
15. Nellis GF, Abdo AY, Engelstad RL, Cotte EP. Theoretical analysis of 157-nm hard pellicle system purification via a cyclic purge/fill process. *J Micro/Nanolith MEMS MOEMS*. 2004;3(1):122–129.
16. Yao J, Wang H, Dittler R, Geisert C, Shadman F. Application of pressure-cycle purge (PCP) in dry-down of ultra-high-purity gas distribution systems. *Chem Eng Sci*. 2010;65(17):5041–5050.
17. Williams E, Ayres R, Heller M. The 1.7 kilogram microchip: energy and material use in the production of semiconductor devices. *Environ Sci Technol*. 2002;36(24):5504–5510.
18. Verma NK, Haider AM, Shadman F. Contamination of ultrapure systems by back-diffusion of gaseous impurities. *J Electrochem Soc*. 1993;140(5):1459–1463.
19. Dittler R, Kishore J, Geisert C, Shadman F. Contamination of ultra-high-purity (UHP) gas distribution systems by back diffusion of impurities. *J IEST*. 2014;57(1):63–76.
20. Barnard A, Hunt W, Timlake W, Varley E. A theory of fluid flow in compliant tubes. *Biophys J*. 1966;6(6):717–724.
21. Churchill SW. Friction-factor equation spans all fluid-flow regimes. *Chem Eng*. 1977;84(24):91–92.
22. Bird RB, Stewart WE, Lightfoot EN. *Transport Phenomena*, *2nd ed*. New York: Wiley, 2006.
23. U.S. Army Corps of Engineers. Engineering and Design Liquid Process Piping. Dept. of the Army, Engineering Manual No.1110-1-4008; 1999.
24. Juneja H, Yao J, Shadman F. Effect of sampling line characteristics on the dynamic monitoring of fluid concentrations. *Ind Eng Chem Res*. 2009;48(11):5481–5488.
25. Gakheladze LR, Gelashvili GV, Mdivnishvili MO, Nanobashvili IS, Nanobashvili SI, Rostomashvili GI. Shock wave propagation in gases under subatmospheric pressure. *Czechoslovak J Phys*. 1999; 49(6):993–997.

Manuscript received Mar. 4, 2015, and revision received May 12, 2015.